Grain-boundary free energy in an assembly of elastic disks

Mark T. Lusk*

Division of Engineering, Colorado School of Mines, Golden, Colorado 80401, USA

Paul D. Beale[†]

Department of Physics, University of Colorado, Boulder, Colorado 80309, USA

Grain-boundary free energy is estimated as a function of misorientation for symmetric tilt boundaries in an assembly of nearly hard disks. Fluctuating cell theory is used to accomplish this since the most common techniques for calculating interfacial free energy cannot be applied to such assemblies. The results are analogous to those obtained using a Leonard-Jones potential, but in this case the interfacial energy is dominated by an entropic contribution. Disk assemblies colorized with free and specific volume elucidate differences between these two characteristics of boundary structure. Profiles are also provided of the Helmholtz and Gibbs free energies as a function of distance from the grain boundaries. Low angle grain boundaries are shown to follow the classical relationship between dislocation orientation/spacing and misorientation angle.

I. INTRODUCTION

The bulk, thermodynamic properties of hard disk and sphere assemblies have been considered for more than 80 years [1], and free energies have been estimated both analytically [2–8] and computationally [9–12]. We are not aware of any efforts, though, to characterize the interfacial free energy associated with grain boundaries in such systems. The present work represents a first step along this path through the consideration of symmetric tilt boundaries in periodic assemblies of near hard elastic disks.

The grain boundary free energy γ is defined to be the reversible work required to form a unit area of interface between two grains [13]:

$$dU = TdS - PdV + \sum_i \mu_i N_i + \gamma dA. \qquad (1)$$

The following equivalent expressions follow directly from this:

$$
\begin{aligned}
\gamma &= \left. \frac{\partial U}{\partial A} \right|_{S,V,N_i} = \left. \frac{\partial F}{\partial A} \right|_{T,V,N_i}, \\
&= \left. \frac{\partial G}{\partial A} \right|_{T,P,N_i} = \left. \frac{\partial \Omega}{\partial A} \right|_{T,V,\mu_i},
\end{aligned}
\qquad (2)
$$

where U, F, G, and Ω, are the internal energy, Helmholtz function, Gibbs function, and grand potential, respectively. We consider a periodic NVT system and therefore measure the interfacial free energy in terms of the difference between two Helmholtz values.

For classical solid-state systems, the properties of grain boundaries continue to be an active research topic. The internal energy of a grain boundary at zero temperature can be estimated by a single, static relaxation. The grain-boundary internal energy is the difference between the energy of the relaxed state and that of a perfect crystal at zero temperature. Finite temperature thermodynamic properties of grain boundaries are more difficult to estimate computationally. Thermodynamic integration techniques must start at a state for which the boundary is fully characterized and follow a path that avoids all bulk and boundary phase transitions [11,12]. Alternatively, estimates may be constructed using a self-consistent *local harmonic approximation* to efficiently estimate grain-boundary free energies [14–17]. In classical systems, however, the entropic contribution (TS) to grain-boundary free energy is relatively small and can sometimes be disregarded. For instance, this entropic contribution is estimated to be no more than 16% for [001] twist boundaries in gold [17], and bicrystal, molecular dynamics simulations can be used to measure the grain-boundary internal energy at constant temperature and zero pressure [18].

Most of these approaches are applicable only to systems governed by an attractive potential. In an assembly of hard disks a local harmonic approximation is not reasonable, and the prominently figuring entropic component of free energy cannot be disregarded. In fact, for a system of hard disks, the grain-boundary Helmholtz free energy is shown to be purely entropic—i.e., it is simply the negative of the product of temperature and interfacial entropy. Thermodynamic integration techniques might be adapted to study grain boundaries in such assemblies, but this is computationally intense, must contend with grain-boundary phase transitions, and has not yet been attempted to the best of our knowledge.

In this paper we present a method for estimating the thermodynamic properties of steric grain boundaries using the concept of free volume. The method is used to quantify the grain-boundary free energy as a function of misorientation for a two-dimensional tilt boundary associated with nearly hard, elastic disks.

---

*Electronic address: mlusk@mines.edu

[†]Electronic address: Paul.Beale@Colorado.edu

II. HOMOGENEOUS ASSEMBLIES OF DISKS

A. Free volume

A quantity central to our work is the free volume associated with each disk. In an assembly of densely packed, hard disks, the free volume of a given disk is simply the area that the center of the disk sweeps out in exploring all its possible configurations while holding all other disks fixed. For systems governed by a pair potential $u(\vec{r}_1, \vec{r}_2)$, the potential energy of a single disk at $\vec{r}_1$ is given by

$$\Phi(\vec{r}_1) = \sum_{i \neq 1} u(\vec{r}_1, \vec{r}_i),$$

where, again, all other disks are held fixed. The free volume v_f is then defined as

$$v_f = e^{-\beta \Phi_0/2} \int \vec{dr}\, e^{-\beta[\Phi(\vec{r}) - \Phi_0]} \tag{3}$$

where $\beta = 1/kT$ and Φ_0 is the potential energy of the disk when it is in its equilibrium position [2]. The free volume of each disk in an assembly is determined using Monte Carlo integration. However, for a homogeneous assembly of evenly spaced, hard disks, the free volume of each disk, $v_f^{(H)}$, can be determined analytically [23]:

$$\frac{v_f^{(H)}}{\sigma^2} = \frac{3a^2\sqrt{3}}{2} - \frac{3a}{2}\sqrt{4 - a^2} - 6 \arcsin\left(\frac{a}{2}\right) + \pi. \tag{4}$$

Here

$$a\sigma = \sqrt{\frac{2}{\rho\sqrt{3}}} \tag{5}$$

is the distance between disk centers expressed in units of σ, the diameter of one disk, and ρ, the number density.

B. Simple cell theory

In cell theory, the partition function for a homogeneous assembly of disks is approximated by [2]

$$Q^{(sc)} = \Lambda^{-2N}(v_f^{(H)})^N \tag{6}$$

where, as usual, $\Lambda = h\sqrt{\beta/(2\pi m)}$ is the mean thermal wavelength. With the Helmholtz function denoted by F, the reduced Helmholtz free energy per unit disk, $f^{(sc)*} = \beta F/N$, can be written as a function of the free volume:

$$f^{(sc)*} = \frac{-1}{N}\ln[Q^{(sc)}] = 2\ln\left[\frac{\Lambda}{\sigma}\right] - \ln\left[\frac{v_f^{(H)}}{\sigma^2}\right]. \tag{7}$$

It is convenient to work with the excess Helmholtz free energy per disk, the configurational contribution to the free energy:

$$f^{(sc)} = f^{(sc)*} - 2\ln\left[\frac{\Lambda}{\sigma}\right] = -\ln\left[\frac{v_f^{(H)}}{\sigma^2}\right]. \tag{8}$$

Then the pressure is given by

$$\frac{\beta P^{(sc)}}{\rho} = \rho\frac{df^{(sc)}}{d\rho} = \frac{-\rho}{v_f}\frac{dv_f^{(H)}}{d\rho}. \tag{9}$$

Equations (4), (5), and (9), provide a means of estimating the thermodynamic properties of a homogeneous assembly of disks using simple cell theory. In the high density limit, simple cell pressure is well approximated by the so called crystal equation of state [19]:

$$\frac{\beta P^{(crys)}}{\rho} = 1 + \frac{1}{\sqrt{\rho_{max}/\rho} - 1}, \tag{10}$$

where

$$\rho_{max} = \frac{2}{\sqrt{3}}, \quad \rho_{min} = 1.080\,68 \tag{11}$$

gives the range of number density over which the assembly is in the solid state. This pressure relation can be integrated to give an approximation to the Helmholtz function valid at high densities. Using $df/d\rho = \beta P/\rho^2$, the excess Helmholtz free energy per disk is

$$f^{(crys)} = -2\ln\left(-1 + \sqrt{\frac{\rho_{max}}{\rho}}\right) - 0.9531. \tag{12}$$

The integration constant is determined using the free energy of the simple cell theory associated with Eq. (4).

C. Fluctuating cell theory

In an attempt to improve on simple cell theory, Hoover *et al.* [7,8] considered an average of the free volumes of each disk associated with thermal fluctuations of the surrounding cage of neighboring disks, so that Eq. (8) is replaced by

$$f^{(fc)} = -\ln\left[\frac{\langle v_f\rangle}{\sigma^2}\right]. \tag{13}$$

Equation (3) is then used to calculate the free volume of each disk numerically. For a homogeneous assembly, the temporal and ensemble averages may be interchanged, so that the disk positions at a single time can be used to estimate the excess Helmholtz free energy:

$$f^{(fc,H)} = -\ln\left[\sum_{i=1}^{N}\frac{v_{f,i}}{N\sigma^2}\right]. \tag{14}$$

Within the homogeneous setting, the fluctuating cell method actually provides an estimate for the Helmholtz function that is not as good as that of the simple cell theory. As will be shown, however, there appears to be a simple relationship between the simple cell and fluctuating cell measures of free
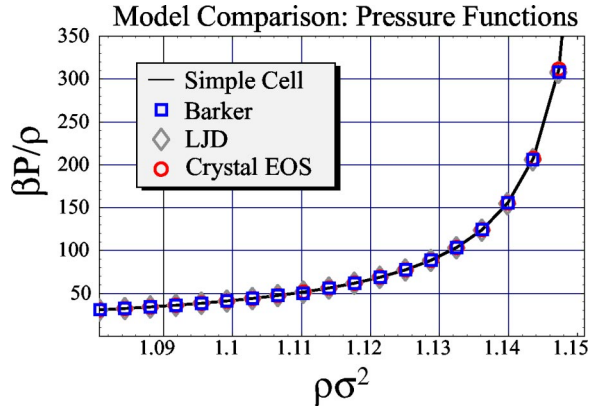
FIG. 1. Comparison of pressure functions for simple cell theory: Barker, Lennard-Jones/Devonshire, and the crystal equation of state.

FIG. 2. Simple cell free volume of a single disk in a hexagonal cage is calculated using Eq. (3) and Monte Carlo integration. The result is plotted as a function of elastic stiffness K. As K increases, the free volume approaches that predicted by Eq. (4).

volume that can be exploited, so that the fluctuating cell method gives free energy estimates that are as accurate as the simple cell approach. Thus calibrated, the fluctuating cell method can be applied to assemblies that are not homogeneous—in particular, to consider the free energy associated with a grain boundary.

D. Other approaches

The thermodynamics of hard disk assemblies have been estimated using a variety of free volume methods, but we include the results of just two approaches for comparison with both the simple cell method and our own numerical calculation of bulk properties. In both cases, free volume formulas are offered in place of Eq. (4). Barker [5,6] applied the Bethe approximation [20], also known as the quasichemical approximation [21], to obtain

$$f^{(B)} = -\ln\left[\frac{v_f^{(B)}}{\sigma^2}\right],$$

$$\frac{v_f^{(B)}}{\sigma^2} = \left(\frac{a-1}{0.5231}\right)^2, \tag{15}$$

while Salsburg et al. [22] used a simple cell approach to give

$$f^{(S)} = -\ln\left[\frac{v_f^{(S)}}{\sigma^2}\right],$$

$$\frac{v_f^{(S)}}{\sigma^2} = \left(\frac{a-1}{0.5373}\right)^2. \tag{16}$$

Figure 1 compares the pressure for these two methods with the results of simple cell theory and the crystal equation of state.

E. Application of the fluctuating cell method to homogeneous assemblies

A molecular dynamics (MD) model was developed and used to study the thermodynamics of the elastic disk assemblies. The pair potential used is

$$u(\vec{r_1}, \vec{r_2}) = \frac{K}{2}(|\vec{r_2} - \vec{r_1}| - 2\sigma)^2 \tag{17}$$

for $|\vec{r_2} - \vec{r_1}| < 2\sigma$ and zero otherwise. A Verlet algorithm was used to integrate the equations of motion, periodic boundary conditions were enforced, and both the volume and temperature were held constant. The temperature was maintained by periodically normalizing the total kinetic energy.

The simulation was nondimensionalized using disk mass m, disk diameter σ, and characteristic time τ. Disks were given an initial velocity with components randomly chosen between $-20\sigma/\tau$ and $20\sigma/\tau$. For an infinite, hard disk assembly, this fixes $\beta = 1/(kT) = 0.0075\tau^2/(m\sigma^2)$. The stiffness parameter K was set so that $\beta K\sigma^2 = 3e^7$. As shown in Fig. 2, this gives fluctuating cell free volumes that are within 2% of those predicted by simple cell theory for hard disks. The data for this plot were generated in association with a single disk caged by six neighbors on a hexagonal lattice. Equation (4) was used to calculate the free volume numerically, and Eq. (4) was used to generate the asymptote.

As has been reported elsewhere, the effect of finite size on free volume follows a $\ln(N)/N$ decay, and this is shown in Fig. 3. The results were used to establish a minimum assembly size of 2000 disks for all simulations used estimate grain-boundary free energy.

Calibration of the fluctuating cell method

It would seem reasonable to suppose that the average value of the fluctuating cell free volume would be the simple cell free volume, but this is not the case [10,23,24]. This issue was investigated using 17 periodic assemblies of 2500 disks having densities that ranged from 1.08 (near the fluid limit) to 1.15 (near the close-packed limit). The fluctuating
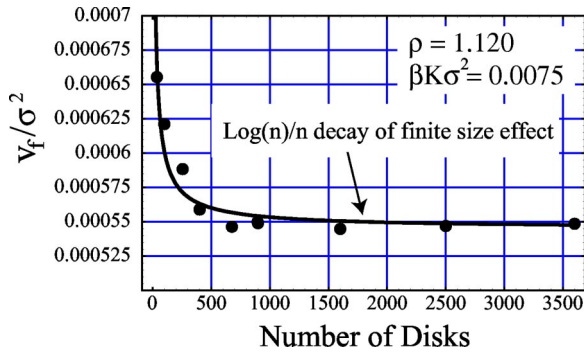
FIG. 3. Finite size effect for homogeneous assemblies of nearly hard disks. Fluctuating cell theory and Monte Carlo integration were used to calculate the average free volume of nine assemblies of varying sizes.

cell free volume was then measured for each disk and these values were normalized using the simple cell free volume formula of Eq. (4). The results, shown in Fig. 4, indicate that the normalized size distributions do not vary with density and have, collectively, an average value of 0.673. The normalized simple cell value is, of course, 1.00, so the free volume from fluctuating cell theory must be multiplied by 1.486 in order to obtain the simple cell value.

This calibration issue was further investigated to see how the calibration factor varies with number density with the results summarized in Fig. 5. As is clear from the plot, the ratio of fluctuating cell and simple cell free volumes is essentially constant up to a number density of 1.12. From there it falls off, and this is most likely due to errors in fluctuating cell free volume measurement takes into account the disk elasticity while the simple cell model does not. The high density results were therefore disregarded in calculating a final calibration factor of 1.502 (see Fig. 6). Such a constant calibration factor amounts to a vertical shift of the Helmholtz free energy, as shown in Eq. (13).

With a calibration in place, the Helmholtz free energy can be estimated using the fluctuating cell method and compared with the analytical predictions of simple cell theory of Eq. (4), the crystal equation of state, the Bethe approximation of
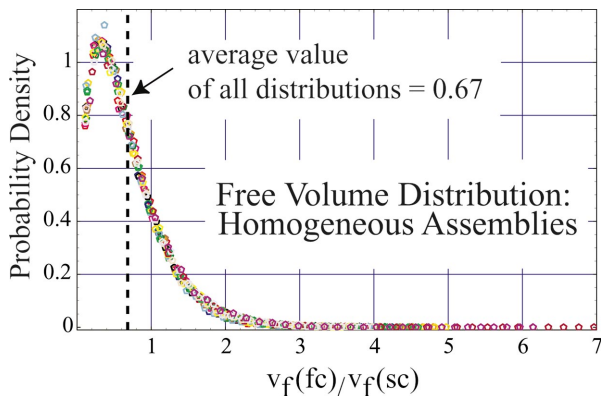
FIG. 4. (Color) Histogram of free volumes for 17 homogeneous assemblies covering a number density of 1.08 to 1.15. The results of each simulation were normalized by the simple cell free volume for the associated number density.
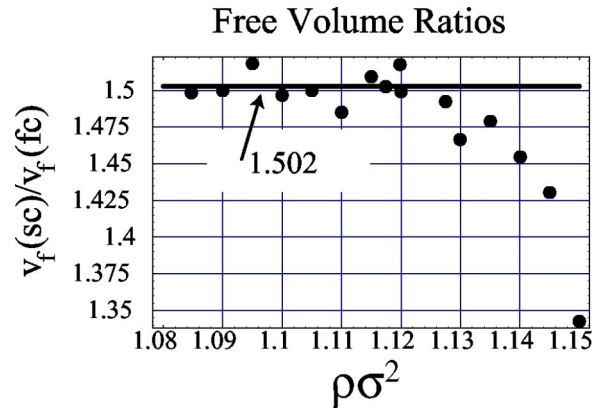
FIG. 5. The ratio of free volumes as predicted by simple cell theory and as measured by fluctuating cell theory. The solid line is at a ratio=1.502.

Barker, and simple cell approximation of Salsburg *et al*. Simulations were run with 2500 disks at the temperature and elastic stiffness prescribed above. Five time slices were considered for each assembly, so the average free volume estimates were based on 12 500 individual free volume calculations. The results shown in Fig. 7 indicate that the free energy calculated using the calibrated fluctuating cell model is consistent with the four other approaches. A basic premise of this work is that the fluctuating cell method can be applied to inhomogeneous distributions of disks as well as being a means of estimating the grain boundary free energy.

III. MODELING SYMMETRIC TILT BOUNDARIES

An algorithm, summarized in the following steps, was developed to determine tilt boundaries that give a periodically repeating structure in both directions. Given a hexagonal lattice with one of the close-packed directions aligned vertically, find all disks a distance X from the lower left disk, where $49\sigma \leqslant X \leqslant 51\sigma$. Draw a line between one of the disks and the lower left disk. The angle between this line and the horizontal is $\theta/2$—i.e., one-half of the grain-boundary tilt angle that will have a horizontal period of X. From this set of angles, select a subset for which a line can be drawn at an angle of $\pi/2 - \theta/2$ from the origin to a disk located at a distance $45\sigma \leqslant Y \leqslant 100\sigma$. This subset of angles will have a
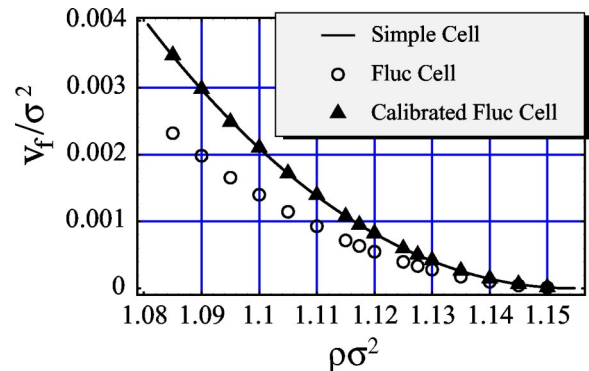
FIG. 6. Calibration of the fluctuating cell method using simple cell theory. A fitted calibration ratio of 1.502 was used.
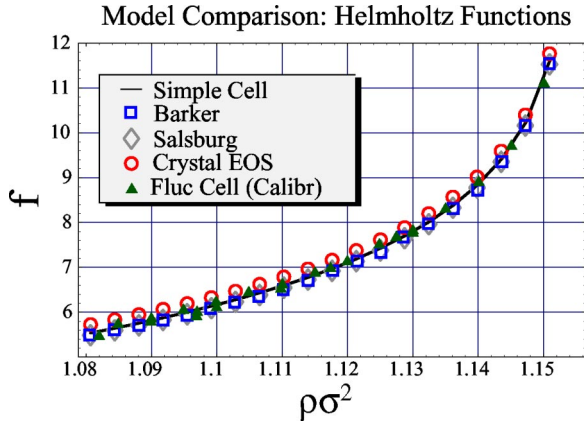
FIG. 7. The Helmholtz free energy functions of simple cell theory of Eq. (4), the Bethe approximation of Barker, the simple cell approximation of Salsburg, and the crystal equation of state compared with the free energy estimate of the calibrated fluctuating cell method. The fluctuating cell data was generated using assemblies with 2000 disks and five time slices, so the free volume estimates were based on the average free volume of 10 000 disks.

vertical period of Y for the tilted grain. Figure 8 illustrates this idea. There are 55 misorientation angles distributed in a relatively even manner in the range $0 \le \theta < 60°$.

Within the periodic domain, bicrystals were constructed with two vertical tilt boundaries as shown in Fig. 9.

For each bicrystal, three simulations were performed. After allowing for the system to reach a dynamic equilibrium, five time slices were chosen from the first two simulations, and ten time slices were chosen from the third simulation (which was twice as long). For each of these time slices, the free volume of each disk was calculated. An average free volume was obtained by constructing 51 vertical bins—each with a width of one disk diameter. For a given angle of bicrystal misorientation and a given bin, the average free volume within the bin was calculated using all 20 time slices. It was implicitly assumed, therefore, that each disk within a given bin is in a state that might be achieved by any other disk in the same bin. This seems reasonable since the bin boundaries are parallel to the grain boundaries. Equation (13) was then used to derive the excess Helmholtz free energy of
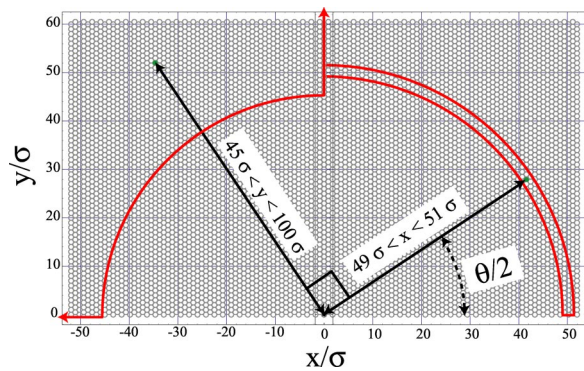
FIG. 8. Illustration of the algorithm for choosing angles for symmetric tilt boundaries such that the horizontal and vertical domains are periodic.
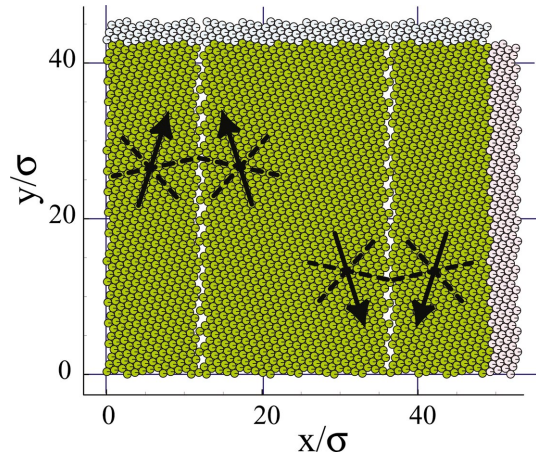
FIG. 9. (Color) Initial condition for a symmetric tilt boundary system with a misorientation of 35.56°. Portions of the upper and right periodic replicas are shown to illustrate that the algorithm used makes a perfect match on all periodic boundaries.

the assembly by adding up the contribution from all bins:

$$f_i^{(\text{fc})} = - N_i \ln \left[\frac{\langle v_f \rangle_i}{\sigma^2} \right]. \tag{18}$$

The thermal average was taken over the 20 time slices chosen.

The binning data for free volume and Helmholtz free energy were supplemented with data for the average specific volume v_i for each disk within bin i. This is the average space assigned to each disk and is equal to the inverse of the number density ρ; it was calculated using a Voronoi algorithm [25]. The specific volume allows an estimate to be made of the average Gibbs free energy per disk associated with each bin:

$$g_i^{(\text{fc})} = f_i^{(\text{fc})} + P v_i. \tag{19}$$

The pressure P is obtained from the crystal equation of state, Eq. (10), using the average number density of the disks associated with the bulk phases.

A typical result is shown in Fig. 10 and illustrates the way in which these quantities vary along a line perpendicular to the grain boundaries. Within the hard disk, *NVT* ensemble, the temperature and internal energy are the same with and without grain boundaries. The spatial variation in the Helmholtz function is therefore due to the fact that disks within the grain-boundary region have a higher entropy than those within the bulk. The figure also shows a horizontal line at the value of Helmholtz free energy for the assembly without any grain boundaries. Grain-boundary formation clearly causes the Helmholtz free energy of the bulk disks to go up while decreasing the free energy of the disks in the vicinity of the boundaries. The rise in the bulk Helmholtz energy offsets the decrease in the Helmholtz energy associated with the grain boundaries, and so the total Helmholtz free energy of the assembly is higher with grain boundaries than without.

As indicated by Eq. (2), the increase in the Helmholtz free energy of the bulk is a consequence of maintaining a con-
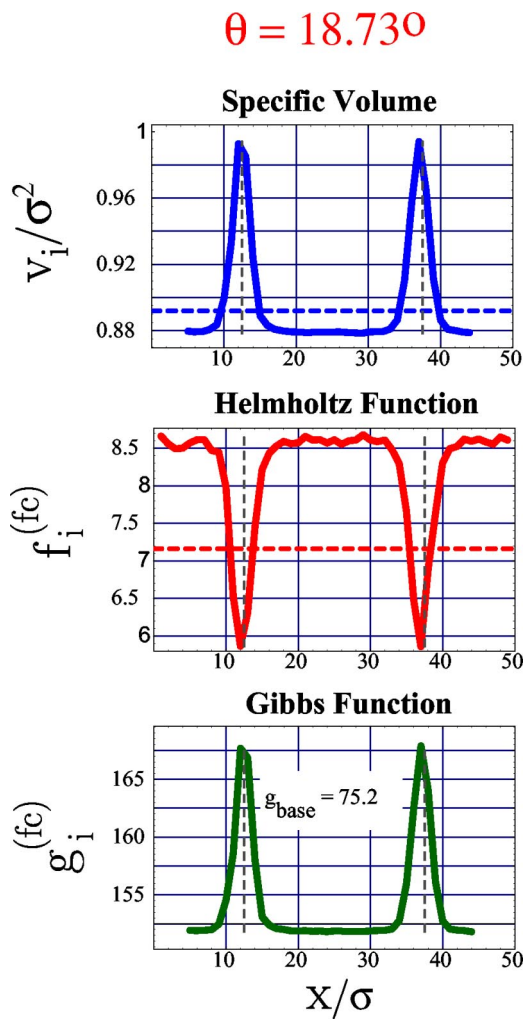
FIG. 10. A typical Helmholtz free energy profile in the assembly. The dashed line indicates the excess Helmholtz free energy per disk for a homogeneous assembly of the same number density. Note that the Helmholtz free energy within the grain boundaries decreases while the overall Helmholtz function increases.
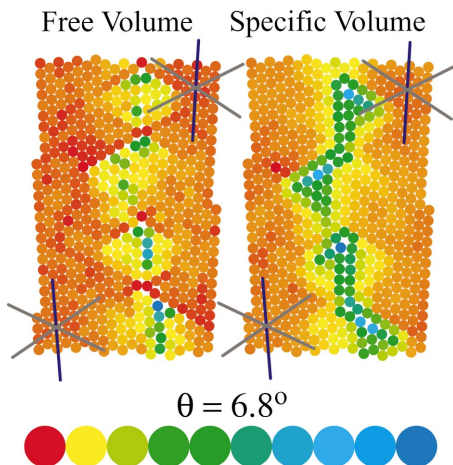
FIG. 11. (Color) Low angle grain boundary.
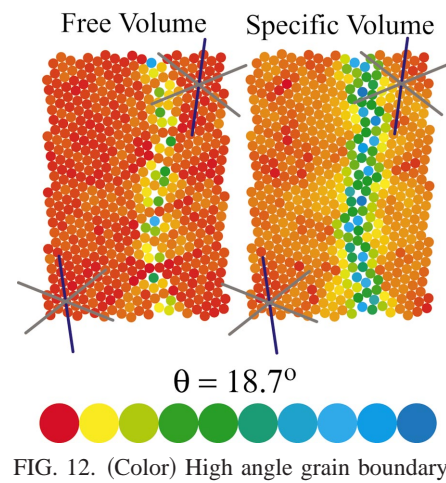
FIG. 12. (Color) High angle grain boundary.
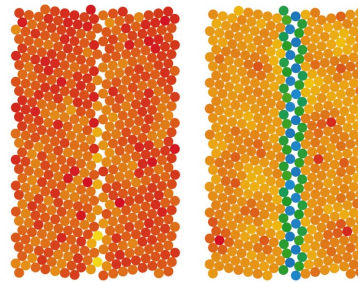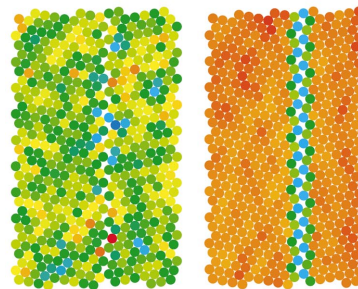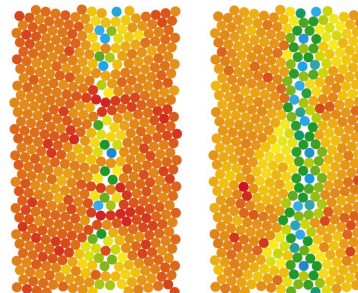
FIG. 13. (Color) Transition through the $\Sigma 7$ coincidence site lattice, showing how the structure of the free volume and specific volume vary with position across grain boundaries.

Specific Volume

Helmholtz Function

Gibbs Function

Vertical Bin

— 37.8° — 38.2° + 40.0°
(~Σ7)
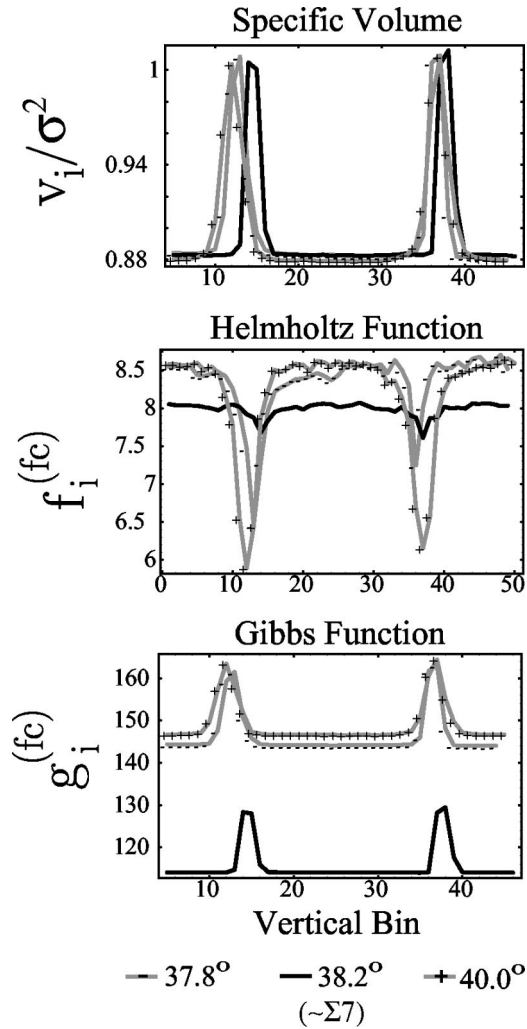
FIG. 14. Transition through the Σ7 coincidence site lattice, showing how specific volume, Helmholtz free energy, and Gibbs free energy vary with position across grain boundaries.

stant volume. The formation of a grain boundary therefore causes the system pressure to increase while the specific volume of the bulk decreases. These effects combine in the Gibbs function to give a localized picture of the grain-boundary free energy. If the Gibbs free energy of the assembly is compared with that of a homogeneous assembly at the same final pressure, the change in free energy is localized to the grain boundary. This is shown in Fig. 10. The spikes in the Gibbs function reflect the increase in free energy of an isobaric, isothermal assembly due to the presence of grain boundaries. Formation of an identical grain boundary within a larger assembly will give a different grain-boundary energy, though, because the final pressure of the system will be lower. Grain-boundary formation for sufficiently large assemblies may be viewed as isobaric, but this is not the case for the assemblies of the current study.

IV. GRAIN-BOUNDARY STRUCTURE

For each of the 55 misorientations considered, the grain-boundary structure was plotted by using color maps of the free and specific volume of each disk. These images offer structural information that is lost in the binning algorithm. The hues are associated with the average values of volume for all 20 time slices mapped onto positions associated with one arbitrary time slice. Each plot is individually normalized so as to best exhibit relative variations. As is typical in atomic bicrystals, the grain-boundary structure exhibits a spatial periodicity that increases with misorientation. The packets merge at misorientations near 15°. Typical low and high angle grain boundaries are shown in Figs. 11 and 12.

The most pronounced difference between free and specific volume plots is the 38.2° boundary of Fig. 13—very nearly a Σ7 boundary. The free volume shows almost no variation between bulk and boundary disks while the specific volume exhibits a spike across grain boundaries that is similar to that of boundaries that are not coincidence site lattices. A very similar result is obtained for a misorientation of 21.787°—close to the other Σ7 boundary.

The color plots can be compared with the binning data shown in Fig. 14, where it is clear that the three misorientations have a nearly identical variation in specific volume. However, the Σ7 boundary exhibits a strikingly homogeneous free volume, implying that the bulk and grain-boundary disks have almost the same Helmholtz free energy for the coincidence site lattice (CSL). This is shown in the second plot and is in sharp contrast to the large variation in the Helmholtz function for misorientations that are only slightly different. The third plot shows that the Gibbs free energy of the Σ7 boundary is much lower than that of the non-CSL grain boundaries, but the relative heights of the grain-boundary spikes are the same.

At misorientation angles close to either 0° or 60° the grain boundaries are composed, as expected, of regularly spaced dislocations. This is highlighted for two cases in Fig. 15.

As with classical solid-state systems, the dislocation orientation and spacing can be related to the misorientation angle [26]. The relations are

$$\theta|_{\text{near } 0°} = 2 \sin^{-1}\left(\frac{b\cos(30°)}{2D}\right),$$

$$\theta|_{\text{near } 60°} = 60 - 2\sin^{-1}\left(\frac{b}{2D}\right), \tag{20}$$

and the table below indicates that these provide reasonable approximations to the misorientation angles for several of the grain boundaries simulated. Input for the estimated angles was obtained by counting the spacing between dislocations.

$\theta^°_{\text{actual}}$	$\theta^°_{\text{estimate}}$
3.48	3.42
4.56	4.51
5.80	5.52
51.9	52.64
53.99	53.98
55.95	56.11

$\theta = 3.48^o$ $\theta = 56.03^o$

Specific Volume
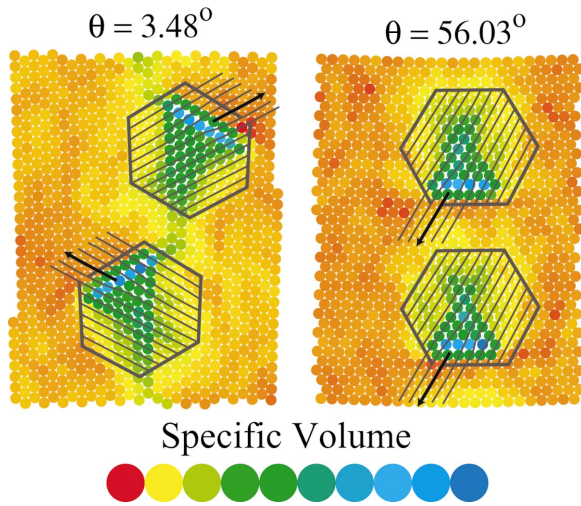
FIG. 15. (Color) Low angle grain boundaries are composed of a series of dislocations, but the structure is different for misorientations near 0° (left) than near 60° (right).

Free Volume   Specific Volume

$\theta = 51.9^o$

FIG. 16. (Color) Bridging networks in the free and specific volumes are typical of most grain boundaries but are particularly clear in this 51.9° misorientation.

As the misorientation between grains moves from these extremes, individual dislocations can no longer be discerned. However, regular patterns still exist in both the free volume and specific volume color plots, and these are qualitatively distinct. Most of the free volume plots clearly show a periodic pattern demarcated by disks that bridge adjacent grains without exhibiting a free volume different than that associated with the bulk disks. Free volume bridges are in a different state of stress than adjacent regions within the grain boundary and may play a dominant role in the transfer of force from one grain to another. This is similar to the jamming and force chain phenomena observed in colloidal suspensions of hard particles [27]. These features are illustrated in Fig. 16 for a misorientation of 51.9°. Bridging is also clear in the high angle boundary of Fig. 12 and in the third pair of boundaries of Fig. 13.

Grain boundaries typically contain disks with free volumes much larger than those associated with the bulk. This can be seen in the color plots of Figs. 11, 12, and 13 and, via Eq. (13), through the Helmholtz function profiles of Figs. 10

and 14. This suggests that the distribution of free volumes is most likely different between bulk and interfacial disks. In order to quantify this, the histograms were constructed of the collective free volume for each bin for 500 grain boundary simulations covering the 55 tilt boundary misorientations. Three such bin histograms are shown in Fig. 17.

Bins located symmetrically on either side of the right grain boundary were found to have essentially the same free volume distribution as that of the homogeneous assemblies of Fig. 4, while bins that included the grain-boundary region exhibit a much wider variation in free volumes. In fact, this transition was found to vary smoothly as a function of bin location. The grain-boundary distribution also includes a long tail out to free volumes a factor of 200 times that of the simple cell prediction. This tail is not shown in order to more easily see that the distributions away from grain boundaries have essentially no free volumes with a relative value greater than 4.

The grain boundary distribution in free volumes shown in Fig. 17 is derived from 55 misorientations and suggests that there is a general nature to the free volume distribution of inhomogeneously packed disks that is exhibited by considering a wide range of such packings via tilt boundaries. With
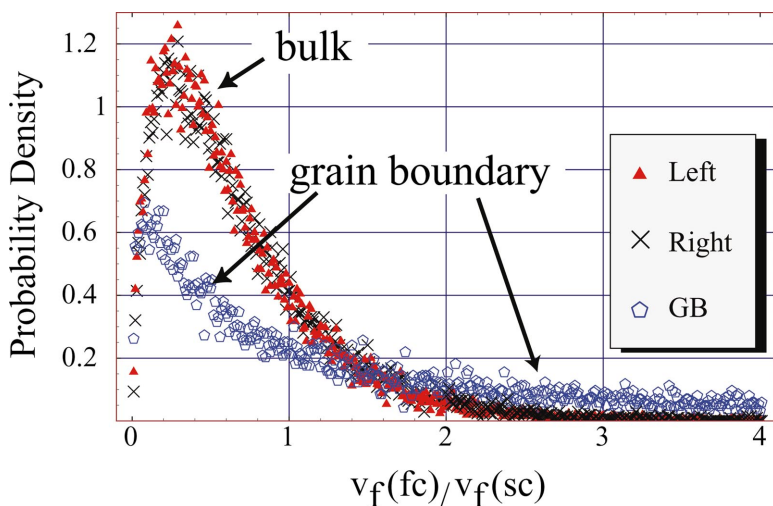
FIG. 17. (Color) Free volume distributions for three vertical bins based on 500 simulations covering all 55 misorientations. The two similar distributions (red and black) are $+7$ and -7 bins from the right grain boundary, while the lower, wider distribution is for a bin coincident with the boundary itself.

the exception of a very rapid rise near zero free volume, this distribution shows an exponential decay in probability density with increasing free volume, and it is likely that the rapid rise for very small free volumes is associated with disk elasticity and would not be present for disks that were truly hard. This effect was already noted in the discussion on fluctuating cell calibration associated with Fig. 5. Interestingly, a similar exponential distribution is observed in free volumes of assemblies of pairs of fused hard disks [28].

V. GRAIN-BOUNDARY FREE ENERGY AS A FUNCTION OF MISORIENTATION

The Helmholtz free energy of each bin can be added in order to obtain the total Helmholtz free energy as a function of misorientation angle. In particular, Eq. (18) was used to derive the excess Helmholtz free energy of each assembly:

$$f^{(\text{fc})} = \sum_{i=0}^{50} f_i^{(\text{fc})} = -\sum_{i=0}^{50} N_i \ln\left[\frac{\langle v_f \rangle_i}{\sigma^2}\right]. \tag{21}$$

Since the domain size V is known for each bicrystal, the simple cell result of Eq. (8) can be used to calculate the Helmholtz function without any interface:

$$f_H^{(\text{fc})} = -N \ln\left[\frac{v_f^{(H)}}{\sigma^2}\right]. \tag{22}$$

Here the homogeneous free volume $v_f^{(H)}$, a function only of number density $\rho = N/V$, was obtained using Eqs. (4) and (5). For the simulations, the initial state of the assembly was constructed such that the average number density was fixed at $\rho = 1.120\,44$. Using Eq. (2), the dimensionless grain-boundary free energy is then

$$\beta\sigma\gamma = \frac{\beta(f^{(\text{fc})} - f_H^{(\text{fc})})}{2h/\sigma}. \tag{23}$$

Here h is the height of the domain, and the factor of 2 is required because there are actually two grain boundaries contributing to the change in the Helmholtz function. Note that Eqs. (21), (22), and (3) imply that, for an assembly of hard disks, the right-hand side of Eq. (23) is not a function of temperature. Since the grain-boundary entropy is defined as $S_{\text{gb}} = -(\partial\gamma/\partial T)|_{N,V}$, the grain-boundary free energy is just

$$\gamma = -TS_{\text{gb}} \tag{24}$$

in the limiting case of hard disks—i.e., the free energy is purely entropic. In an assembly of nearly hard, elastic disks, this is the dominant contribution to the grain-boundary free energy, and in the hard disk case it is the only contribution. This term is often neglected in solid-state systems.

Figure 18 shows the final plot of interfacial free energy as a function of misorientation for symmetric tilt boundaries.

Of particular interest was whether or not coincidence site lattices exhibit distinctive free energies in the same manner as for classical solid-state grain boundaries [29–31]. All four $\Sigma 7$ and $\Sigma 13$ boundaries show dips in the grain-boundary
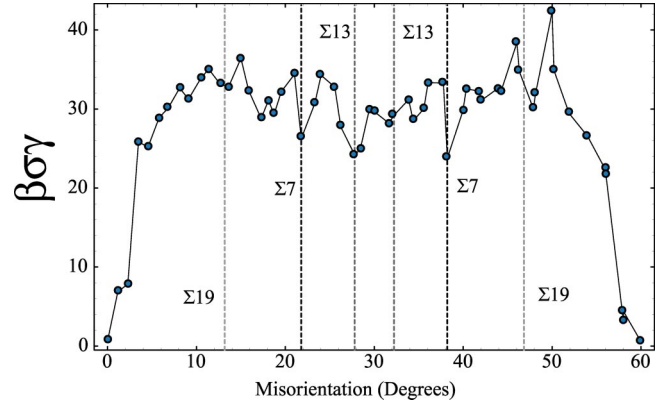
FIG. 18. The interfacial free energy of an assembly of nearly hard, elastic disks is plotted as a function of misorientation.

free energy with, possibly, small dips for the $\Sigma 19$ boundaries as well. As far as we are aware, this plot represents the first estimate of grain-boundary free energy as a function of misorientation for any steric system. These results can be compared with the energy plot of Fig. 19 obtained for a two-dimensional system governed by a Lennard-Jones pair potential:

$$\Phi(r_{ij}) = \varepsilon\left[\left(\frac{r_0}{r_{ij}}\right)^{12} - 2\left(\frac{r_0}{r_{ij}}\right)^{6}\right]. \tag{25}$$

Periodic, zero pressure boundary conditions were enforced and isothermal conditions maintained. A half-loop, bicrystal geometry was used, so that any dependence on interface orientation was averaged. The entropic contribution was assumed to be negligible [18].

Two alternate methods for estimating grain-boundary free energy

The result obtained for grain-boundary free energy is based on a binning strategy in which the free energy of ver-
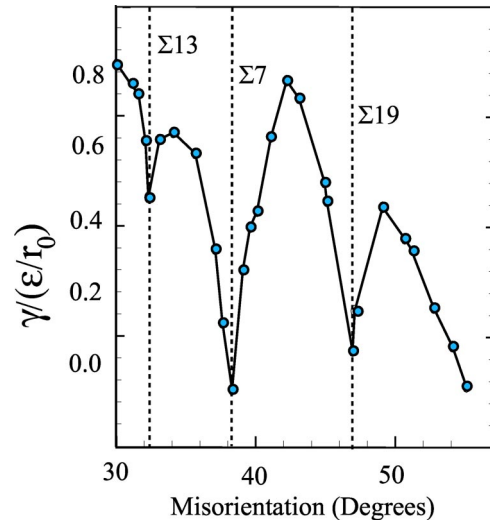
FIG. 19. Molecular dynamics prediction of the variation in grain boundary internal energy with misorientation for a tilt boundary. A Lennard-Jones potential was used for the two-dimensional system.

tical slices of the assembly is calculated using the average free volume of disks in each bin. An implicit assumption is that the average free volume of disks in a bin represents the thermally averaged free volume of any one disk in that bin. In addition, the measured free volume of each disk is multiplied by a correction factor of 1.502 in order to better match the free volumes of homogeneous assemblies. Alternatives to the binning approach and the free volume calibration factor were also considered as explained below. These other approaches were considered because the application of fluctuating cell theory to inhomogeneous assemblies has not been justified, and it was thought that other strategies of accounting for assembly inhomogeneity might lead to different free energy results. However, the alternate methods were found to give essentially the same results as the original method, and this lends a measure of support for the application of fluctuating cell theory to assemblies with grain boundaries.

The vertical binning strategy can be replaced by an approach that groups disks according to their free volume instead of lateral position. The underlying assumption behind such a strategy is that disks with a similar free volume represent configurations that any one such member of the group will eventually find itself in. As has already been discussed in association with Fig. 17, grain-boundary structures were found to be relatively stable and typically had a number of disks which maintained a stable free volume that was many times greater than that of the disks in the bulk. Removal of these larger disks from the calculation results in a renormalized distribution that is more closely aligned with that of the bulk and suggests that some improvement in the free energy estimate might be obtained by treating the larger disks separately. Disks were therefore binned according to size with a bin dividing point at $v_f^{(\text{fc})}/v_f^{(\text{sc})}=4$:

$$f^{(\text{fc},H)} = -\frac{1}{N}\left(N_{\text{small}}\ln\left[\frac{\langle v_f\rangle_{\text{small}}}{\sigma^2}\right] - N_{\text{large}}\ln\left[\frac{\langle v_f\rangle_{\text{large}}}{\sigma^2}\right]\right).$$

An analysis showed that this free energy estimate was not sensitive to variations in the cutoff size between 3 and 5. This equation was used in place of Eq. (14) to generate a plot of grain-boundary free energy.

A third method was also considered that is based on a different way of calibrating the fluctuating cell algorithm. Rather than calibrating the average fluctuating cell free volume of a homogeneous assembly to that predicted by simple cell theory, a calibration could be made in order to match the bulk free energies of the two assemblies—i.e.,

$$f^{(\text{sc})} = f^{(\text{fc},H)},$$

where Eq. (14) is replaced by

$$f^{(\text{fc},H)} = -\frac{1}{c_f N}\sum_{i=1}^{N}\ln\left[\frac{v_{f,i}}{\sigma^2}\right]. \tag{26}$$

Here c_f is the calibration factor that must be provided to match the free energies. Using the same approach as in the calibration of free volumes, it was found that $c_f = 1.11$ gave the best match between simple cell and fluctuating cell free energies of homogeneous assemblies. This value and Eq. (26) were then used to estimate the grain-boundary free energy as a function of misorientation with the same data used to produce Fig. 18.

The two alternative methods of calculating free energy were found to give essentially the same results to that of the original method shown in Fig. 18. This implies that the features of this plot are not tied to either the vertical binning strategy or the free volume averaging scheme.

VI. CONCLUSIONS

Molecular dynamics can be used to estimate the interfacial free energy and structure of symmetric tilt boundaries in assemblies of nearly hard disks. The most common techniques for obtaining interfacial free energy rely on an attractive component to the pair potential and cannot be applied to such systems. Fluctuating cell theory was therefore used to estimate the interfacial free energy and was calibrated for homogeneous assemblies using simple cell theory. An algorithm was developed to identify symmetric, tilt boundaries for which both vertical and horizontal periodicity is maintained, and simulations were performed on 55 of these special angles. This was sufficient to construct a plot of interfacial free energy as a function of tilt boundary angle in assemblies of nearly hard, elastic disks. The structure of these grain boundaries was also studied through a comparison of free volume and specific volume plots. It was shown that the low angle boundaries obey classical kinematic rules and are composed of a series of dislocations. The free energy of individual dislocations was not quantified, but this will be undertaken. Grain boundaries typically exhibited volume bridging—periodically occurring bridges of disks with volumes the same as those associated with their bulk counterparts. Also of interest was that both $\Sigma 7$ boundaries showed a large jump in specific volume across grain boundaries with no corresponding jump in free volume.

Now that the interfacial free energy of symmetric tilt boundaries has been estimated as a function of misorientation, it should be possible to use MD simulations to quantify the mobility of curvature driven grain boundaries. A plot analogous to that of Fig. 18 could be developed for this mobility.

The use of a MD simulation was originally motivated by an interest in studying the kinetics of grain boundaries in deforming, lightly dissipative assemblies. It should also be possible, though, to estimate the interfacial free energy using a Monte Carlo simulation and thermodynamic integration from an Einstein bicrystal. Such an approach, while more computationally intense, would allow the consideration of truly rigid disks and would offer an independent check on the results presented here. The thermodynamic integration results, currently being pursued by our group, would be particularly useful in evaluating the application of fluctuating

cell theory to inhomogeneous assemblies—the primary assumption of this investigation. It would also be useful to consider an isobaric, isothermal ensemble with the Monte Carlo setting in order to develop a plot of the Gibbs free energy as a function of misorientation with the same pressure for each misorientation angle [32]. This is not possible in the constant volume setting, since each misorientation is associated with a different pressure.

---

[1] P.W. Bridgman, Phys. Rev. **3**, 126 (1914); **3**, 153 (1914).

[2] J.E. Lennard-Jones and A.F. Devonshire, Proc. R. Soc. London, Ser. A **163**, 53 (1937).

[3] F.H. Stillinger, Z.W. Salsburg, and R.L. Kornegay, J. Chem. Phys. **43**, 932 (1965).

[4] F.H. Stillinger and Z.W. Salsburg, J. Chem. Phys. **46**, 3962 (1967).

[5] J.A. Barker, J. Chem. Phys. **63**, 632 (1975).

[6] J.A. Barker and H.M. Gladney, J. Chem. Phys. **63**, 3870 (1975).

[7] W.G. Hoover, W.T. Ashurst, and R. Grover, J. Chem. Phys. **57**, 1259 (1972).

[8] W.G. Hoover, N.E. Hoover, and K. Hansen, J. Chem. Phys. **70**, 1837 (1979).

[9] W.G. Hoover and F.H. Ree, J. Chem. Phys. **47**, 4873 (1967).

[10] W.G. Hoover and F.H. Ree, J. Chem. Phys. **49**, 3609 (1968).

[11] D. Frenkel and A.J.C. Ladd, J. Chem. Phys. **81**, 3188 (1984).

[12] D. Frenkel and B. Smit, *Understanding Molecular Simulation: From Algorithms to Applications* (Academic, New York, 1996).

[13] J.W. Cahn, in *Interfacial Segregation*, edited by W.C. Johnson and J.M. Blakely, Vol. 3 (ASM International, Metals Park, OH, 1979).

[14] A.P. Sutton, Philos. Mag. A **60**, 147 (1989).

[15] R. LeSar, R. Najafabadi, and D.J. Srolovitz, Phys. Rev. Lett. **63**, 624 (1989).

[16] R. Najafabadi, D.J. Srolovitz, and R. LeSar, J. Mater. Res. **5**, 2663 (1990).

[17] R. Najafabadi, D.J. Srolovitz, and R. LeSar, J. Mater. Res. **6**, 999 (1991).

[18] M. Upmanyu, R.W. Smith, and D.J. Srolovitz, Interface Sci. **6**, 41 (1998).

[19] F.H. Stillinger and Z.W. Salsburg, J. Stat. Phys. **1**, 179 (1969).

[20] H.A. Bethe, Proc. R. Soc. London, Ser. A **150**, 552 (1935).

[21] R.H. Fowler and E.A. Guggenheim, Proc. R. Soc. London, Ser. A **174**, 189 (1940).

[22] Z.W. Salsburg, W.G. Rudd, and F.H. Stillinger, J. Chem. Phys. **47**, 4353 (1967).

[23] S.C. Gay, P.D. Beale, and J.C. Rainwater, J. Chem. Phys. **109**, 6820 (1998).

[24] J.A. Barker, *Lattice Theories of the Liquid State* (Pergamon, New York, 1963).

[25] F.P. Preparata and M.I. Shamos, *Computational Geometry* (Springer-Verlag, New York, 1985).

[26] J.P. Hirth and J. Lothe, *Theory of Dislocations*, 2nd ed. (Krieger, Malabar, FL, 1982).

[27] M.E. Cates, J.P. Wittmner, J.P. Bouchard, and P. Claudin, Phys. Rev. Lett. **81**, 1841 (1998).

[28] S.C. Gay, P.D. Beale, and J.C. Rainwater, J. Chem. Phys. **112**, 9841 (2000).

[29] G. Gottstein and L.S. Shvindlerman, *Grain Boundary Migration in Metals* (CRC Press, London, 1999).

[30] A.P. Sutton and R.W. Balluffi, *Interfaces in Crystalline Materials* (Oxford University Press, Oxford, 1996).

[31] F.J. Humphreys and M. Hatherly, *Recrystallization and Related Annealing Phenomena* (Pergamon Press, Oxford, 1995).

[32] M. Parrinello and A. Rahman, J. Appl. Phys. **52**, 7182 (1981).